Geophys. J. R. astr. Soc. (1986) **84,** 185–200

A theoretical and experimental comparison of the anisotropies of magnetic susceptibility and remanence in rocks and minerals

A. Stephenson, S. Sadikun and D. K. Potter *Department of Geophysics and Planetary Physics, School of Physics, The University, Newcastle upon Tyne NE1 7RU*

Accepted 1985 June 19. Received 1985 June 3; in original form 1985 January 28

Summary. Susceptibility, thermo-remanent magnetization (TRM) and isothermal remanent magnetization (IRM) anisotropy ellipsoids have been determined for several rock samples. The results indicate that the ellipsoid of initial susceptibility is less anisotropic than the TRM and low field IRM ellipsoids which are found experimentally to be of identical shape. This suggests that palaeomagnetic data for anisotropic rocks may be corrected by using the anisotropy ellipsoid determined from magnetically non-destructive low field IRM measurements. Such IRM measurements can also be used to obtain anisotropy axes of samples which are inherently anisotropic but which have a susceptibility which is too weak to be accurately measured. The results for a series of artificial anisotropic samples containing magnetite particles of different sizes (in the range 0.2–90 μm) were very similar to those for the rocks. In contrast, a comparison of the susceptibility and IRM ellipsoids for anisotropic samples containing particles from a magnetic tape gave very different results in accordance with theory. Such results imply that susceptibility and IRM ellipsoids could be used to determine whether anisotropic rocks contain uniaxial single-domain particles (magnetization confined to the easy axis) or whether the particles are essentially multidomain.

Key words: Anisotropy, isothermal remanence, magnetic properties of rocks, magnetite, remanent magnetization, susceptibility

1 Introduction

Magnetic anisotropy due to particle alignment is important in palaeomagnetism because it causes the natural remanent magnetization (NRM) vector of rocks to be deflected away from the ambient field vector when the remanence is acquired. Because of its disturbing influence on NRM, anisotropy has been the subject of considerable study – for a review of the subject see Hrouda (1982) – and because of the difficulty in allowing for its effect in computing the original field direction, very anisotropic rocks are often regarded as being unsuitable for palaeomagnetic purposes. A typical upper limit of acceptable anisotropy of susceptibility would be about 5 per cent (i.e. percentage difference between maximum and minimum susceptibilities).

Downloaded from https://academic.oup.com/gji/article/84/1/185/593598 by guest on 21 August 2022

The anisotropy of rocks may be measured in several ways but whatever method is used, the most complete way of specifying it is in terms of an anisotropy ellipsoid. The principal axes of the ellipsoid indicate how anisotropic is the sample and their orientation with respect to the rock indicate the unique axes or planes defined by the physical processes which aligned the magnetic particles when the rock was formed (e.g. flow in a magma, bedding planes of a sediment etc.). It is important to realize, however, that while all methods of measurement are likely to give the same orientation of the anisotropy ellipsoid because of the inherent preferential alignment of the magnetic particles within the rock, the relative magnitudes of the principal axes may differ. Any method of measurement can be used to obtain an anisotropy ellipsoid provided that the magnetization components produced along axes which specify the alignment are linearly proportional to the field components along those axes. Thus initial susceptibility and low field TRM, both of which commonly fulfil this condition (see e.g. Stacey & Banerjee 1974) may be used. As regards the deflection of a TRM from the ambient field direction, while the orientation of the anisotropy ellipsoid relative to the rock is clearly important, the angular deflection will also depend critically on the relative magnitudes of the principal axes. Since it is the TRM ellipsoid which is relevant in this context, incorrect results will be obtained from the susceptibility ellipsoid for example, if this is of different shape.

If a field H is applied with components H'_x, H'_y and H'_z along the principal axes (specified by directions x', y' and z') of the TRM anisotropy ellipsoid, the TRM components acquired along the principal axes will be given by:

$$M'_x = M'_{xx}\, H'_x/H$$

$$M'_y = M'_{yy}\, H'_y/H$$

$$M'_z = M'_{zz}\, H'_z/H \qquad (1)$$

where M'_{xx}, M'_{yy} and M'_{zz} are the principal values of the TRM ellipsoid, i.e. the thermoremanences produced in a field H applied along each axis in turn. Note that M'_{xx}/H etc. may be denoted a 'principal TRM susceptibility'. Once M'_x, M'_y and M'_z are known, the resultant TRM components along the rock coordinates (x, y, z) may easily be found provided that the orientation of the TRM ellipsoid is known. It is thus a simple matter either to compute the TRM vector given the applied field vector or to determine the applied field vector from the TRM vector. If only the shape of the TRM ellipsoid is known (together with its orientation) then only the orientation of the TRM vector or the applied field vector may be computed (not the magnitude). For palaeomagnetic purposes the field magnitude is not usually important so that only the ellipsoid shape and orientation is necessary for the calculation of the original field direction from the measured TRM vector.

Fuller (1963) has compared susceptibility, IRM and TRM anisotropy by applying an appropriate field (which thus produced a corresponding remanence) along the maximum and minimum susceptibility directions. The field used to produce the IRM was 0.2 T and samples containing pyrrhotite showed greater IRM anisotropy than susceptibility anisotropy. Specimens containing hematite (with possible magnetite also) did not show the same consistent difference. In the case of TRM, cooling rocks from above their Curie point in a known magnetic field at 70° to a high susceptibility plane gave a larger divergence of TRM than predicted from the anisotropy of susceptibility (assuming it to be identical to TRM anisotropy). He found that the anomalously high divergence was particularly evident in low susceptibility rocks. Uyeda *et al.* (1963) also report a greater divergence of TRM from the ambient field direction than expected.

Downloaded from https://academic.oup.com/gji/article/84/1/185/593598 by guest on 21 August 2022

In this paper the difference between the anisotropies of TRM and susceptibility is theoretically accounted for and experimental verification of the theory is given.

2 Theoretical relationship between the susceptibility and remanence ellipsoids

Consider an assembly of N_0 particles, each of which has its anisotropy represented by an ellipsoid of revolution. Suppose for simplicity that a fraction k_x' of the N_0 particles is aligned with the principal x'-axis of the sample and fractions k_y' and k_z' with the y' and z'-axes respectively (see Fig. 1).
Thus

$$k_x' + k_y' + k_z' = 1. \tag{2}$$

Let χ_n and χ_p be the susceptibilities of the particle measured normal and parallel to its axis of rotational symmetry respectively and let M_n and M_p be the corresponding remanences (assumed to be proportional to the applied field) acquired by the particle when the field is applied along the respective directions (e.g. a TRM although it could also be an IRM or ARM depending on the acquisition mechanism). Clearly because of the symmetry of the model the principal axes of the susceptibility and remanence ellipsoids of the distribution will coincide. To find the relationship between the magnitude and the shape of the two ellipsoids note that the principal susceptibility measured along the x'-axis in Fig. 1 is given by:

$$\chi_{xx}' = N_0 [k_x' \chi_p + (1 - k_x') \chi_n]. \tag{3}$$

Similar expressions refer to the y'- and z'-axes. Using equation (2) it follows that the sum of the principal susceptibilities χ_t is given by

$$\chi_t = \chi_{xx}' + \chi_{yy}' + \chi_{zz}' = N_0 [\chi_p + 2\chi_n]. \tag{4}$$

Thus k_x' can be expressed as:

$$k_x' = \frac{p_x(\alpha + 2) - 1}{\alpha - 1} \tag{5}$$

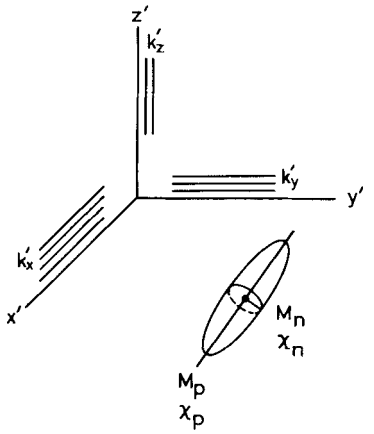

Figure 1. Simple representation of an anisotropic assembly of N_0 particles each of which is an ellipsoid of revolution as shown. k_x', k_y' and k_z' represent the fraction which have their easy axes aligned with the x', y' and z'-axes respectively. For an explanation of the other symbols see text.

Downloaded from https://academic.oup.com/gji/article/84/1/185/593598 by guest on 21 August 2022

where

$$p_x = \frac{\chi'_{xx}}{\chi_t} \text{ and } \alpha = \frac{\chi_p}{\chi_n}. \tag{6}$$

Similar expressions give p_y and p_z. p_x, p_y and p_z are thus normalized principal susceptibilities describing the shape of the susceptibility ellipsoid of the rock and represent the relative lengths of the principal axes of an ellipsoid which is of average dimension $\chi_t/3$. Note that $p_x - 1/3$ etc. represent departures from isotropy and

$$p_x + p_y + p_z = 1. \tag{7}$$

A similar argument can be used for TRM giving the result that

$$k'_x = \frac{q_x(\gamma + 2) - 1}{\gamma - 1} \tag{8}$$

where

$$q_x = \frac{M'_{xx}}{M_t} \text{ and } \gamma = \frac{M_p}{M_n}. \tag{9}$$

M'_{xx} and M_t are the corresponding expressions for remanence and are obtained from (3) and (4) by replacing χ'_{xx}, χ'_{yy}, χ'_{zz}, χ_t, χ_p, χ_n by M'_{xx}, M'_{yy}, M'_{zz}, M_t, M_p and M_n respectively. M'_{xx}, etc. are thus the principal axes of the TRM ellipsoid. Equating (5) and (8) gives, for the rock:

$$p_x = p_0 + sq_x \tag{10}$$

(similarly for p_y and p_z) where

$$p_0 = \frac{\gamma - \alpha}{(\alpha + 2)(\gamma - 1)} \tag{11}$$

and

$$s = \left(\frac{\alpha - 1}{\alpha + 2}\right)\left(\frac{\gamma + 2}{\gamma - 1}\right) = (1 - 3p_0). \tag{12}$$

Equation (10) predicts that if the relative dimensions of the principal axes of the susceptibility ellipsoid of the rock are plotted against those of the TRM ellipsoid the points (q_x, p_x), (q_y, p_y), (q_z, p_z) should lie on a straight line passing through the point (1/3, 1/3) with intercept p_0 and slope s. Note that percentage susceptibility anisotropy = percentage TRM anisotropy $\times$ $|s|$ where percentage anisotropy is defined as $100 \times$ (max–min axis) $\div$ average. If $0 < p_0 < 2/3$ (i.e. $|s| < 1$) then the susceptibility ellipsoid will be less anisotropic than the remanence ellipsoid and if $p_0 > 1/3$ then the slope of the p versus q graph is negative and the maximum susceptibility axis corresponds with the minimum TRM axis. Only if $\gamma = \alpha$ (i.e. $p_0 = 0$, $s = 1$) will the two ellipsoids be of identical shape. Equations (10–12) are generally applicable to any anisotropic distribution of non-interacting anisotropic particles and thus by determining p_0 or s, individual particle characteristics (the relationship between α and γ) can be related to anisotropy measurements on samples. α and γ in turn are dependent on the laws governing the susceptibility and TRM acquisition of the anisotropic particle parallel and normal to its axis of rotational symmetry.

To examine further the relationship between the anisotropy of the rock and the character-

Downloaded from https://academic.oup.com/gji/article/84/1/185/593598 by guest on 21 August 2022

istics of the particles within it, it is useful to make the following definitions:

$$\alpha_p = \frac{\alpha}{\alpha + 2} = \frac{\chi_p}{\chi_0} : \alpha_n = \frac{1}{\alpha + 2} = \frac{\chi_n}{\chi_0} \tag{13}$$

$$\gamma_p = \frac{\gamma}{\gamma + 2} = \frac{M_p}{M_0} : \gamma_n = \frac{1}{\gamma + 2} = \frac{M_n}{M_0} \tag{14}$$

where $\chi_0 = \chi_p + 2\chi_n$ and $M_0 = M_p + 2M_n$. α_p and α_n thus represent the normalized particle susceptibilities parallel and perpendicular to the axis of rotation of the particle respectively (see Fig. 1). They are thus the normalized axes of the susceptibility ellipsoid of the particle. γ_p and γ_n similarly represent the normalized principal TRM values of the particle. Using equations (10–12) it can be shown that:

$$\alpha_p = p_0 + s\gamma_p \tag{15}$$

and

$$\alpha_n = p_0 + s\gamma_n. \tag{16}$$

Equations (15) and (16) thus show that a plot of the normalized principal susceptibilities and TRM values of the particle gives the same line as the plot of the normalized principal susceptibility and TRM values of the rock (equation 10). Although the points (γ_p, α_p), (γ_n, α_n) relating to the individual particles cannot be uniquely determined from the plot of the rock parameters p against q (equation 10), they must lie on the same line. (It can also be shown that the parameters for a particle with three unequal axes also lie on this line.) Since

$$\alpha_p + 2\alpha_n = \gamma_p + 2\gamma_n = 1 \tag{17}$$

it follows that given the limits of α_p or γ_p, the limits of α_n or γ_n can also be set, and since from equations (13) $\alpha = 2\alpha_p/(1 - \alpha_p)$, the limits of α can also be set (similarly for γ). Thus from inspection of Fig. 2, if $0 < p_0 < 0.5$ then $0 < \gamma_p < 1$ and α_p must lie between p_0 and

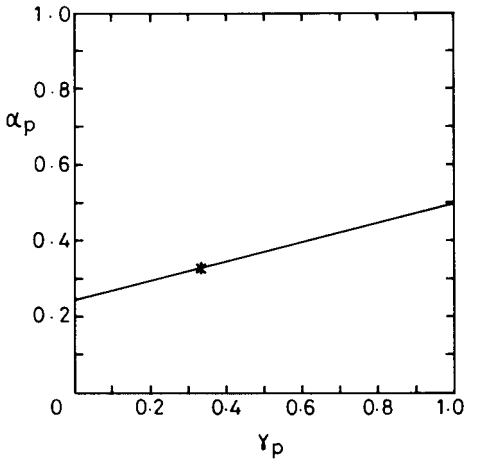

Figure 2. The dependence of the normalized principal susceptibility α_p of a particle (measured along its rotation axis) on the corresponding normalized principal TRM (γ_p) of the particle given along the same direction for an intercept p_0 of 0.25 derived from a hypothetical plot of p against q for a rock according to equation (10). The possible range of γ_p is $0 < \gamma_p < 1$ and α_p is thus constrained for this example to lie between 0.25 and 0.5. A negative intercept would set a constraint on possible values of γ_p since in that case $0 < \alpha_p < 1$. The point (γ_n, α_n) also lies on this line. The star * is at (1/3, 1/3).

Downloaded from https://academic.oup.com/gji/article/84/1/185/593598 by guest on 21 August 2022

$1-2p_0$. If $p_0 > 0.5$ then $0 < \gamma_p < p_0/(3p_0 - 1)$ and $0 < \alpha_p < p_0$. Finally if p_0 is negative $0 < \alpha_p < 1$ and $-p_0/(1 - 3p_0) < \gamma_p < 1 + 2p_0/(1 - 3p_0)$.

Thus anisotropy measurements on rocks can yield information about the properties of the individual particles which they contain and enable constraints to be set against which theories of TRM acquisition and susceptibility can be tested. Fig. 2 illustrates how the range of the particle parameter α_p may be found from measurements of the susceptibility and TRM anisotropy ellipsoids of a rock.

It should be noted that although the distribution discussed here is very simplified it does give results (equations 10–16) which turn out to be identical to those obtained from a more realistic distribution, namely one in which the density of easy axes per unit solid angle $n(\theta, \phi)$ varies according to the equation

$$n(\theta, \phi) = \frac{3N_0}{2\pi} \left[k_z' + (k_y' - k_z') \sin^2 \theta + (k_x' - k_y') \sin^2 \theta \cos^2 \phi\right] \tag{18}$$

(Stephenson 1981), where θ and ϕ are spherical polar coordinates defined in the usual way, i.e. θ is the polar angle (co-latitude) and ϕ is the azimuth angle (longitude) – (in Stephenson 1981 these are interchanged). N_0 is the total number of particles in the distribution. k_x' here is the number density along the x'-axis multiplied by $2\pi/(3N_0)$. Similar definitions apply to k_y' and k_z'. Owens (1974) has also discussed the susceptibility of anisotropic distributions of particles.

3 Calculation of intercept p_0 for multidomain particles

Stacey (1963) has given an expression for TRM (M) in weak field (H) for a large multidomain particle of strongly magnetic material such as magnetite. This is

$$M = \frac{HI}{N(1 + N\chi_i)} \tag{19}$$

where $I[= M_s(T_B)/M_s(0)]$ is the ratio of the spontaneous magnetization at the blocking temperature T_B to that at room temperature. N is the demagnetizing factor and χ_i is the intrinsic susceptibility. Thus

$$\gamma = \frac{M_p}{M_n} = \frac{N_n(1 + N_n\chi_i)}{N_p(1 + N_p\chi_i)} \tag{20}$$

where the subscripts p and n refer to directions which are parallel and normal to the axis of the particle as before. The apparent susceptibility of such a particle is given by

$$\chi = \frac{\chi_i}{1 + N\chi_i} \tag{21}$$

and thus

$$\alpha = \frac{\chi_p}{\chi_n} = \frac{1 + N_n\chi_i}{1 + N_p\chi_i}. \tag{22}$$

Thus p_0 can be calculated as a function of say N_n and χ_i (since $N_p = 1 - 2N_n$ for a particle which is an ellipsoid of revolution). Note that N_n varies from 0 (a disc) through 1/3 (a sphere) to 0.5 (a needle). Fig. 3 shows the calculated results of χ_i against N_n for different values of intercept p_0. Note that for all reasonable values of χ_i and N_n, p_0 lies between 0

Downloaded from https://academic.oup.com/gji/article/84/1/185/593598 by guest on 21 August 2022

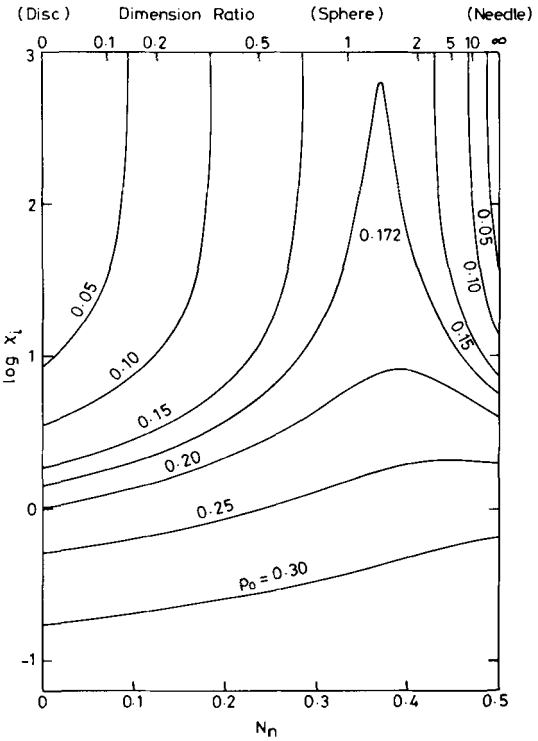

Figure 3. The dependence of intrinsic susceptibility χ_i for a large multidomain particle (which is an ellipsoid of revolution) on the demagnetizing factor N_n (normal to the axis of symmetry) for different values of intercept p_0. The dimension ratio (axial ÷ transverse) is also shown.

and 1/3. This means that the slope of the p, q graph as given by equation (10) is positive and less than 1 and thus on the basis of Stacey's theory for multidomain TRM acquisition (a) the anisotropy of TRM should always be greater than that of susceptibility anisotropy (b) the maximum and minimum susceptibility axes of the rock should coincide with the maximum and minimum TRM axes. Note also that for particles which are not too removed from spherical, i.e. dimension ratio between 0.5 and 2 and for intrinsic susceptibilities between 10 and 100 (e.g. large magnetite particles), the intercept p_0 always lies between about 0.12 and 0.20.

4 Calculation of intercept p_0 for single-domain particles

Consider a single-domain grain of uniaxial anisotropy (of revolution) with a single easy axis. In this case the spontaneous magnetization can only lie parallel to the easy axis, i.e. there can be no remanence acquired normal to the axis and thus $M_n = 0$. Thus $\gamma = M_p/M_n = \infty$. Conversely $\alpha = \chi_p/\chi_n = 0$ since the susceptibility measured parallel to the easy axis (and thus to the spontaneous magnetization) is zero. Thus in equation (11) $p_0 = 0.5$ and thus for such particles

$$p_x = 0.5\,(1 - q_x) \tag{23}$$

(similarly for p_y and p_z).

This equation shows that for $q_x > q_y > q_z$ then $p_x < p_y < p_z$ since the p versus q graph

Downloaded from https://academic.oup.com/gji/article/84/1/185/593598 by guest on 21 August 2022

has a slope of -0.5. This means that (a) like the multidomain case, TRM anisotropy is greater than anisotropy of susceptibility, but (b) unlike the multidomain case the maximum and minimum susceptibility axes coincide with the minimum and maximum TRM axes respectively and are thus interchanged. Thus for rocks containing such single-domain grains, the TRM produced in the rock will be deflected away from the maximum susceptibility direction rather than towards it as in the case of multidomain particles.

In the case of a single domain particle which has an easy plane in which the magnetization lies (i.e. the axis of rotation is a 'hard' direction) then $\gamma = M_p/M_n = 0$ since there can be no remanence acquired along the axis. Thus $p_0 = \alpha/(\alpha + 2)$ and is positive. Assuming that $\alpha(=\chi_p/\chi_n)$ is < 1, i.e. the susceptibility within the easy plane χ_n is greater than the susceptibility measured along the axis of symmetry, then $p_0 < 1/3$ and thus for oblate single domain particles (i.e. an easy plane within each grain), TRM and susceptibility maximum and minimum anisotropy axes should coincide, unlike the case for prolate particles. Thus anisotropic samples containing single-domain hematite particles might be expected to give an intercept less than 1/3 since at room temperature the remanence of each particle (if a single crystal) is confined to the basal plane.

5 Experimental determination of the susceptibility and TRM ellipsoids

The susceptibility ellipsoids of a selection of strongly anisotropic rocks consisting of metamorphosed granites, slates and schists were measured on a Digico anisotropy delineator (see Hrouda, Stephenson & Woltär 1983). The TRM ellipsoids of five samples which had anisotropy axes well separated from those marked on the rock (x, y, z) were obtained by heating each sample three times to 700°C and cooling in a field of 84 μT. In the first heating the field was applied along the x-axis and after cooling, the x, y and z components of remanence were measured. In the second and third heatings the field was applied along the y- and z-axes respectively. Thus the following nine values of remanence were obtained

$$\begin{aligned} &M_{xx} \quad M_{xy} \quad M_{xz} \quad \text{(field along } x\text{)},\\ &M_{yx} \quad M_{yy} \quad M_{yz} \quad \text{(field along } y\text{)},\\ &M_{zx} \quad M_{zy} \quad M_{zz} \quad \text{(field along } z\text{)}. \end{aligned} \tag{24}$$

From these nine values, six independent coefficients were obtained, i.e. M_{xx} M_{yy}, M_{zz}, $(M_{xy} + M_{yx})/2$, $(M_{xz} + M_{zx})/2$, $(M_{yz} + M_{zy})/2$. (Theoretically $M_{xy} = M_{yx}$ etc. but to minimize experimental error an average value was taken). These six coefficients were then used in a 'Molspin' anisotropy delineator program which was modified so as to compute the complete TRM ellipsoid, i.e. the magnitudes of the principal axes together with their orientation. (A copy of this (in BASIC) is available on request.) A typical TRM acquired in 84 μT was 2 A m^{-1}, and the off-diagonal terms M_{xy} etc. in (24) were up to 40 per cent (more typically 15 per cent) of the average TRM ($M_t/3$). The average experimental difference between the theoretically identical off-diagonal terms was 4.5 per cent of the average TRM.

There were slight chemical or physical changes produced in the rocks by the heatings as observed by monitoring the low field IRM (in 5 mT) acquired by the rock after each heating. Using the low field IRM to correct the TRM intensities for change did not, however, lead to any significant change in the TRM ellipsoids and so the uncorrected TRM values have been used.

For the five samples studied, the orientation of the room temperature susceptibility and TRM ellipsoids relative to the arbitrary x-, y- and z-axes marked on the rock agreed very

Downloaded from https://academic.oup.com/gji/article/84/1/185/593598 by guest on 21 August 2022

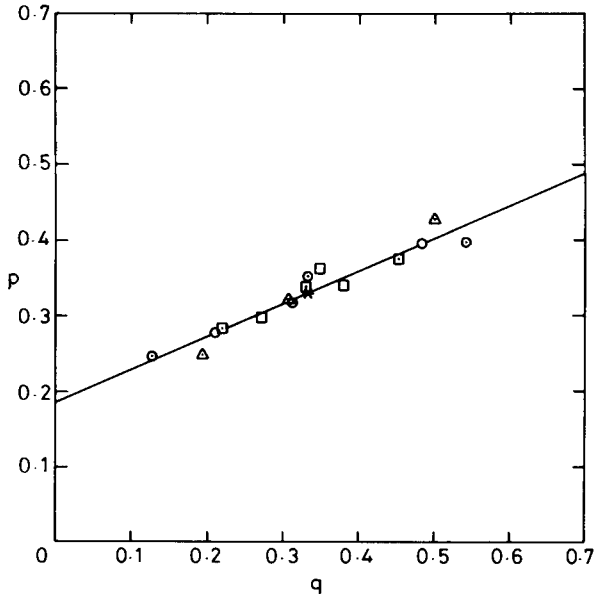

Figure 4. A comparison of the normalized principal axes of the susceptibility ellipsoid (p values) and TRM ellipsoids (q values) for five anisotropic rock samples. For each sample three points are plotted (q_x, p_x), (q_y, p_y) and (q_z, p_z) where $p_x = \chi'_{xx}/(\chi'_{xx} + \chi'_{yy} + \chi'_{zz})$ and $q_x = M'_{xx}/(M'_{xx} + M'_{yy} + M'_{zz})$etc. χ'_{xx} and M'_{xx} etc. refer to principal axes of the susceptibility and TRM ellipsoids respectively. The star * is at (1/3, 1/3).

closely with each other, typically to within a few degrees. Their shapes however, significantly differed from each other and a plot of the normalised principal susceptibilities p_x, p_y, p_z against the corresponding principal TRM parameters q_x, q_y, q_z (see equations 6 and 9) yielded the results of Fig. 4. The plot agrees closely with the theoretical prediction of equation (10) with an average intercept p_0 of about 0.19. Thus for these samples the TRM ellipsoid was more anisotropic than the susceptibility ellipsoid. This result is in agreement with the observations of Fuller (1963) and Uyeda *et al.* (1963) who obtained a larger divergence of TRM than might be expected on the basis of the anisotropy of susceptibility. Note that susceptibilities were typically 30×10^{-3} (SI units), a value which is high enough for the influence of any paramagnetic components to be neglected.

6 Experimental determination of the low field IRM ellipsoid

Janák (1967) has investigated the dependence of the deflection of the IRM vector away from the field direction (in fields between 2.2 and 22 mT) both theoretically (assuming that the IRM vector had the same direction as the vector of induced magnetization in the sample) and experimentally. He found that in most cases there was good agreement between the experimental and calculated deflections although some samples gave considerably higher deflections than allowed by theory. Irving & Park (1973) also investigated the deviation of the IRM vector from the applied field direction. It is thus of interest to compare the low field (5 mT) IRM ellipsoid with that determined by susceptibility measurements. To perform the comparison each rock was given an IRM in a pulse magnetizer which produced a pulsed field of magnitude 5 mT (in this case) and width about 100 ms. The previously af

Downloaded from https://academic.oup.com/gji/article/84/1/185/593598 by guest on 21 August 2022

demagnetized sample (tumbled in 100 mT) was subjected to the pulse along its x-axis, the remanence was measured and the IRM acquired was determined by subtracting from this value any residual remanence left after the 100 mT demagnetization. Thus for the field applied along the x-axis, the components of IRM acquired M_{xx}, M_{xy}, M_{xz} could be determined as for the TRM acquisition described previously. After tumble demagnetization in 10 mT the 5 mT field pulse was applied along the y-axis and then after a subsequent 10 mT demagnetization along the z-axis. Note that theoretically a peak field of 5 mT should be strong enough to tumble demagnetize an IRM acquired in 5 mT (Stephenson 1983) but to ensure complete demagnetization, 10 mT peak was used. The IRM components corresponding to those given in (24) were thus obtained and by using these in the TRM anisotropy ellipsoid program a low field IRM anisotropy ellipsoid could be obtained. It should be pointed out that the equations from which the ellipsoid is calculated make the assumption that remanence is proportional to field (see equation 1). This assumption, while valid for low field TRM (84 μT) is of doubtful validity when applied to low field IRM (5 mT), nevertheless, the orientation of the IRM ellipsoid was the same (to within a few degrees) as for the susceptibility and TRM ellipsoids. Denoting $q_x = \mathrm{TRM}'_{xx}/\mathrm{TRM}_t$ etc. as before and $r_x = \mathrm{IRM}'_{xx}/\mathrm{IRM}_t$ etc. enables a plot of IRM ellipsoid parameters to be made against TRM ellipsoid parameters as in Fig. 5 where the points (q_x, r_x), (q_y, r_y) and (q_z, r_z) are shown for each sample. It is apparent from these results that the two ellipsoids are of virtually identical shape. Thus on the basis of the results for these five samples it would appear that a method of correcting palaeomagnetic data has been found, i.e. the original field direction can be obtained from anisotropic rocks by determining the low field IRM ellipsoid as described above (shape and orientation) and that this can then be used to obtain the required palaeofield direction given the orientation of the NRM vector (assumed to be a TRM acquired after the rock fabric had been imposed).

To illustrate this technique see Figs 6 and 7. Fig. 6 shows the TRM directions for the five

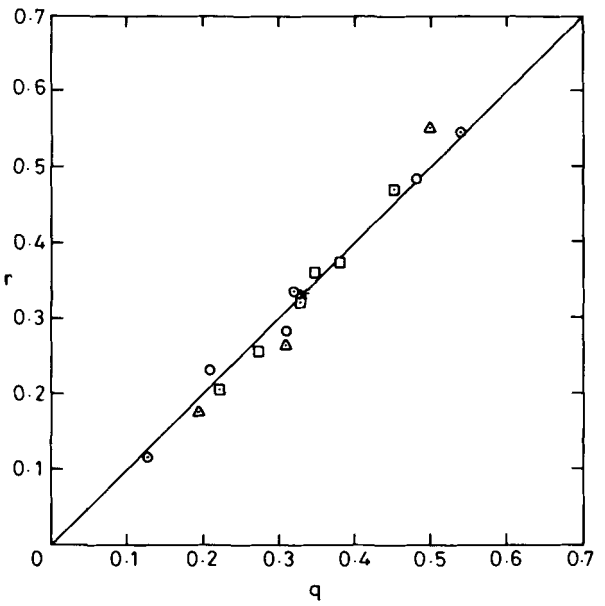

Figure 5. A comparison of normalized principal axes of the IRM ellipsoid (r values) and TRM ellipsoid (q values) for the same five rock samples as in Fig. 4.

Downloaded from https://academic.oup.com/gji/article/84/1/185/593598 by guest on 21 August 2022

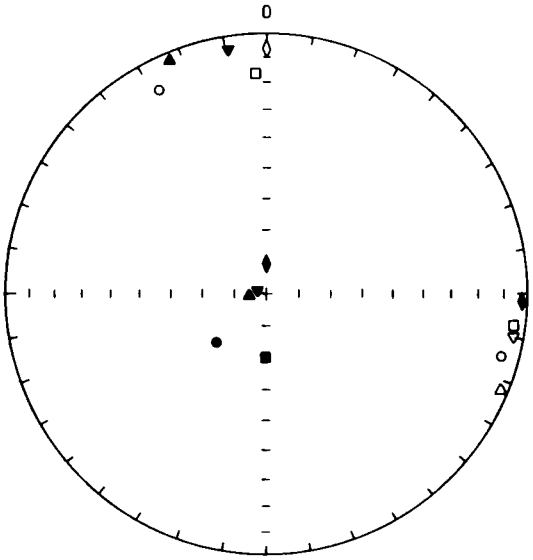

Figure 6. The TRM directions of the five samples of Fig. 4 when they were cooled three times from 700°C in an 84 μT field which was successively applied along the x-, y- and z-axes in turn.

samples when the applied field was aligned in turn with the x-, y- and z-axes respectively. Angular scattering of the TRM vectors up to about 30° away from the field vector is produced by the anisotropies but when the field orientations are computed from the TRM directions using the low field IRM ellipsoid, the scatter is much reduced and the computed directions (Fig. 7) lie very close to those along which the fields were applied, i.e. x, y and z.

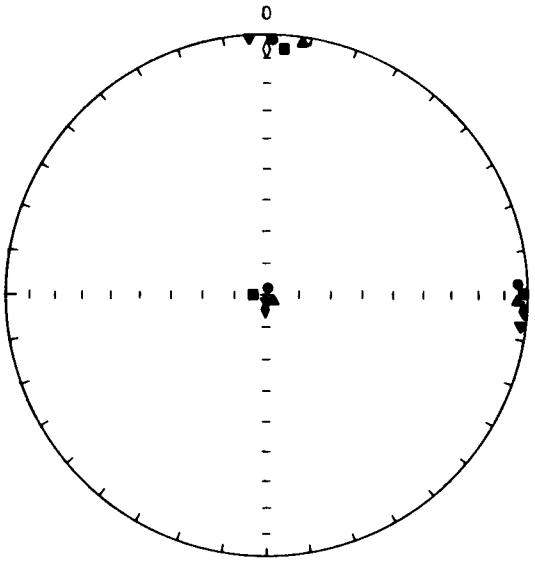

Figure 7. The deduced field directions computed from the TRM directions of Fig. 6 and the low field IRM ellipsoids.

Downloaded from https://academic.oup.com/gji/article/84/1/185/593598 by guest on 21 August 2022

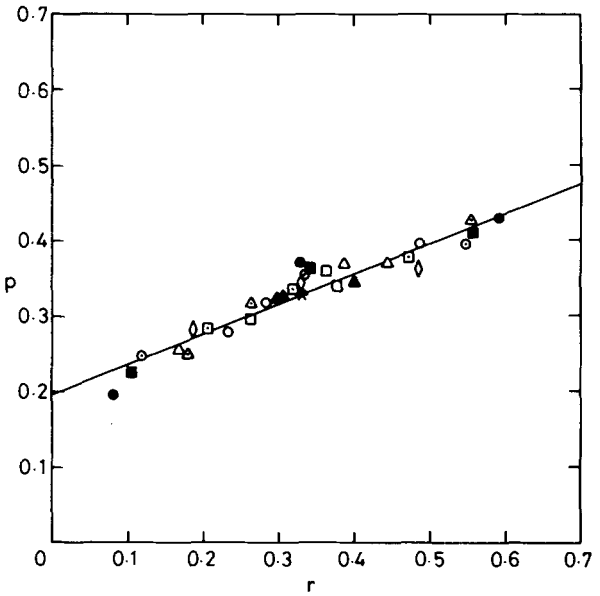

Figure 8. A comparison of the normalized principal axes of the susceptibility (p) and IRM ellipsoids (r) in SmT for 10 rock samples.

7 Comparison of susceptibility and low field IRM ellipsoids for rocks and magnetite samples

Fig. 8 shows the normalized principal susceptibilities p_x, p_y, p_z plotted against the corresponding principal IRM parameters r_x, r_y, r_z for 10 rock samples (including those used in Figs 4 and 5). The intercept p_0 is 0.20 and as expected is very close to that of Fig. 4 because of the apparent equivalence of the TRM and low field IRM ellipsoids.

From the previous theory it would appear that the particles within these rocks (assuming they are of magnetite rather than hematite) are multidomain rather than single-domain because of the observation that p_0 agrees closely with the expected value for multidomain

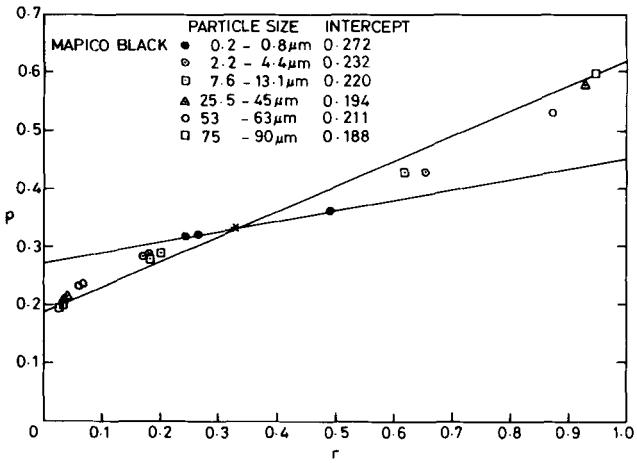

Figure 9. A comparison of the normalized principal axes of the susceptibility (p) and IRM ellipsoids (r) in 5 mT for six different sizes of magnetite particles. The lowest and highest slopes shown refer to the smallest and largest particle sizes respectively.

Downloaded from https://academic.oup.com/gji/article/84/1/185/593598 by guest on 21 August 2022

particles assuming that they are not too prolate or oblate. To test the theory further a series of anisotropic artificial samples containing magnetite of various particle size were made. A Bahco centrifugal dust classifier was used to separate natural magnetite powder into different size fractions. Anisotropic samples were made by mixing the powder with a resin and setting it in the presence of a field of about 50 mT. After tumble-demagnetization, the susceptibility of the samples was measured and their IRM anisotropy ellipsoids (in 5 mT) were obtained as in the previous section. A sample of Mapico black from another source was also included. Fig. 9 shows the results. It is apparent that the intercept for most of the fractions spanning the size range 0.2–90 μm is very close to that for the rocks of Fig. 8 although there is a definite trend in intercept from about 0.19 for the largest particles (which formed the most anisotropic sample) to about 0.27 for the smallest particles (Mapico black). The maximum and minimum slopes are shown in the diagram.

To test whether the shape of the IRM ellipsoid exhibited any dependence on field, one of the fractions (2.2–4.4 μm) had its ellipsoid determined in various fields. These results are shown in Fig. 10. It is clear that there is some dependence on field since the higher the field the less is the apparent anisotropy but any applied field up to about 10 mT would give virtually the same result. Note that in Fig. 10 the values of r_y and r_z are the same because of the way in which the samples were made anisotropic, i.e. the field was applied along the x-axis of the sample during the hardening of the resin so that the final anisotropy is given by an ellipsoid of revolution about the x-axis.

Also shown in Fig. 10 is the variation of the average dimension of the IRM ellipsoid (i.e. $(M'_{xx} + M'_{yy} + M'_{zz})/3$) with applied field. The non-linear behaviour, especially at low fields, does not seem to influence greatly the shape of the anisotropy ellipsoid.

8 Comparison of susceptibility and low field IRM ellipsoids for samples containing single-domain particles

The previous magnetite samples according to the theory of Section 4 do not exhibit any characteristics expected for single-domain particles even though the smallest particles (0.2–0.8 μm) are in the pseudo-single domain range (Dunlop, Stacey & Gillingham 1974). It is

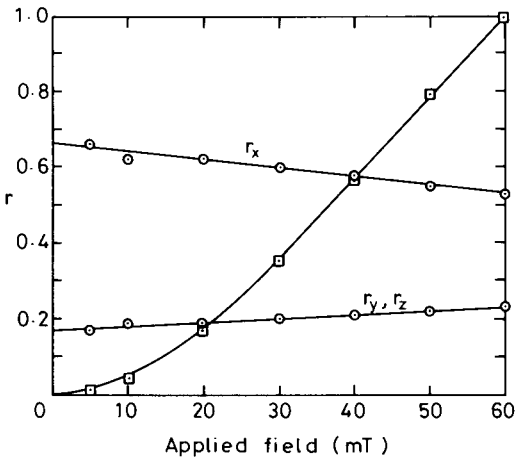

Figure 10. The variation of the normalized principal axes of the IRM ellipsoid as a function of applied field for an anisotropic sample of 2.2–4.4 μm magnetite (circles). Because the ellipsoid had rotational symmetry about the direction (x-axis) of the field which was used to make the sample anisotropic, r_y and r_z are the same. Note that $r_x + r_y + r_z = 1$. The variation of the average ellipsoid size (i.e. $(M'_{xx} + M'_{yy} + M'_{zz})/3$) is also shown (squares). (Actual average in 60 mT is 6.74 Am^2kg^{-1}).

Downloaded from https://academic.oup.com/gji/article/84/1/185/593598 by guest on 21 August 2022

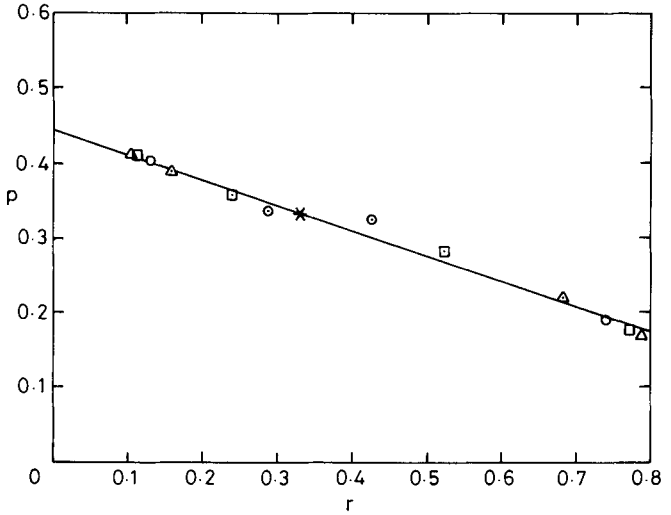

Figure 11. A comparison of the normalized principal axes of the susceptibility (p) and IRM ellipsoids (r) in 60 mT for particles from TDK magnetic tape. The theoretically expected result is an intercept of 0.5.

possible, however, that the increase in intercept from 0.19 to 0.27 as the particle size decreases may be indicative of a change towards single-domain behaviour for which p_0 should be 0.5. To test the theory further a source of single-domain particles was required and so particles from γ-ferric oxide magnetic recording tape (TDK type D) were stripped off the backing material and mixed as homogeneously as possible with resin which was allowed to harden in a magnetic field. Six samples of different anisotropy were made by allowing the resin to harden in different magnetic fields (20–80 mT). Like the magnetite samples, the anisotropies were ellipsoids of rotation with the axis of symmetry coincident with the field direction. This axis (x) had the lowest susceptibility. Results for the susceptibility and IRM ellipsoid parameters are shown in Fig. 11. Because the y- and z-axes of both ellipsoids were almost identical, an average value of these together with the x parameters (r_x, p_x) is plotted in Fig. 11, i.e. there are only two points plotted per sample. Note that the field used to obtain the IRM ellipsoid was 60 mT since the 5 mT used for the previous experiments was so much smaller than the anisotropy field of the particles that no remanence was acquired. A least squares fit for the six samples gives an intercept of 0.45. Although this differs from the expected value of 0.5, nevertheless as predicted by theory, the maximum and minimum axes of the susceptibility ellipsoid no longer coincide with the maximum and minimum axes of the IRM ellipsoid as for multidomain particles but are interchanged. The slightly lower intercept than expected might suggest that the particles are not competely single-domain. Alternatively it may be due to some other factor not being taken into account by the simple model used. In the case of the tape samples it is quite possible that the particles were not completely separated and that clumps of interacting particles still distributed in a plane were present. This might modify the result.

An anisotropic sample fabricated from natural hematite (44–76 μm) gave an intercept of about 0.2.

9 Conclusions

The results and theory described in this paper may be summarized as follows.

(a) An IRM ellipsoid may be determined by applying a field along the x-, y- and z-axes in turn as described earlier and measuring the nine components of magnetization produced.

Downloaded from https://academic.oup.com/gji/article/84/1/185/593598 by guest on 21 August 2022

This method is particularly useful in obtaining anisotropy axes of samples which are inherently anisotropic but where the susceptibility is too weak to be accurately measured. Since it is an anisotropy of remanence it will not be influenced by any paramagnetic or superparamagnetic contribution to the susceptibility which would even further reduce the anisotropy of the susceptibility ellipsoid compared to the TRM or IRM ellipsoids.

(Although not studied in this paper an ARM ellipsoid can also in principle be determined in a similar way to the TRM and IRM ellipsoids by applying the steady field along each of the axes in turn and tumbling the sample and magnet system used to produce the steady field in a high alternating field (Stephenson & Collinson 1974). The alternative method of giving the sample a longitudinal ARM (steady and alternating fields coincident) along each of the three axes in turn could lead to the production of a GRM (Stephenson 1980) in addition to the ARM, and the disturbing effect of this could be serious for weak applied steady fields.)

(b) The low field IRM ellipsoid for the five rock samples studied is the same shape as the TRM ellipsoid determined by giving each sample a TRM along its x-, y- and z-axes in turn and measuring the nine components of TRM produced.

(c) The susceptibility ellipsoid is in general of quite different shape from the IRM or TRM ellipsoids and when the normalized susceptibilities (p_x, p_y, p_z) are plotted against the normalized principal axes of the IRM or TRM ellipsoids (r_x, r_y, r_z or q_x, q_y, q_z) the intercept p_0 on the p-axis can indicate whether or not the particles in the anisotropic sample are prolate single-domain or multidomain. Note however that single-domain particles can only be detected via IRM measurements if the applied field is comparable to the anisotropy field of the particles, i.e. fields of several tens of mT must be applied to detect them.

(d) The IRM ellipsoid, because of its apparent equivalent shape to the TRM ellipsoid, may be used to deduce the direction of the ambient field which produced the NRM (TRM) of rocks. Hence palaeomagnetic pole positions may be found from anisotropic rocks.

It should be noted, however, that, on the basis of the results presented here, this method will be valid only for rocks which contain either multidomain and pseudo single-domain particles down to about 0.2 μm in size (magnetite) or single-domain particles. In the latter case a high field will be required to obtain the remanence ellipsoid whereas in the former case only a low field will be required. For rocks containing a mixture of single-domain and larger grains (PSD or multidomain), incorrect results might be obtained if only a low field is used to obtain the IRM ellipsoid since the single-domain particles within the rock would then be unaffected and not contribute to the IRM. Note, however, that by giving the IRM in a field H and then demagnetizing it in an alternating field of peak value less than H, it should be possible to determine the IRM ellipsoids for particles of different coercivity when a mixture is present. The relative contributions to the overall anisotropy from the single-domain and multidomain particles might thus be estimated.

(e) A determination of the low field susceptibility and high field IRM ellipsoids can indicate whether or not magnetite or titanomagnetite particles within a rock are single domain or multidomain by obtaining the intercept p_0. An intercept near 0.5 would indicate single-domain particles whereas an intercept near 0.2 would indicate pseudo-single domain or multidomain. Note that single-domain hematite particles should not theoretically give an intercept of 0.5 because their magnetization is confined to an easy plane and thus might be expected to give a low intercept. It is possible that detection of the domain type in isotropic rocks could be done by setting magnetically separated particles in resin in the presence of a field so as to produce an anisotropic sample and then using the above method.

(f) A determination of the susceptibility and IRM or TRM ellipsoids for a rock can enable characteristics of the individual particles within it to be determined. In particular,

Downloaded from https://academic.oup.com/gji/article/84/1/185/593598 by guest on 21 August 2022

limits can be defined between which the ratio of susceptibility parallel and perpendicular to the rotation axis of the particles must lie.

(g) The upper limit of about 5 per cent susceptibility anisotropy (difference between maximum and minimum susceptibilities) below which anisotropy is usually considered unimportant for palaeomagnetic purposes could in some cases by very misleading since if $0 < p_0 < 0.67$ susceptibility anisotropy will be less than TRM anisotropy. If p_0 approaches 1/3 then susceptibility anisotropy will be small whereas TRM anisotropy could be very large (e.g. the Mapico Black sample 0.2–0.8 μm in Fig. 9) with a consequent large deviation of the NRM of a rock from the ambient field direction.

Acknowledgments

We wish to thank Dr L. Molyneux for making available the MOLSPIN anisotropy program and the North East Area National Coal Board Scientific Department, and in particular Mr J. Haynes and Mr G. Gray, for their help in preparing the magnetite size fractions. We also thank Dr W. H. Owens who, as a referee, made several valuable suggestions. One of us (DKP) was supported by NERC research grant GR3/4332.

References

Dunlop, D. J., Stacey, F. D. & Gillingham, D. E. W., 1974. The origin of thermoremanent magnetization: contribution of pseudo-single-domain magnetic moments, *Earth planet. Sci. Lett.*, **21**, 288–294.

Fuller, M. D., 1963. Magnetic anisotropy and palaeomagnetism, *J. geophys. Res.*, **68**, 293–309.

Hrouda, F., 1982. Magnetic anisotropy of rocks and its application in geology and geophysics, *Geophys. Surv.*, **5**, 37–82.

Hrouda, F., Stephenson, A. & Woltär, L., 1983. On the standardization of measurements of the anisotropy of magnetic susceptibility, *Phys. Earth planet. Int.*, **32**, 203–208.

Irving, E. & Park, J. K., 1973. Palaeomagnetism of metamorphic rocks: errors owing to intrinsic anisotropy, *Geophys. J. R. astr. Soc.*, **34**, 489–493.

Janák, F., 1967. The effect of anisotropy of magnetic susceptibility on the direction of the vector of isothermal remanent magnetic polarization, *Studia geophys. geol.*, **11**, 419–429.

Owens, W. H., 1974. Mathematical model studies on factors affecting the magnetic anisotropy of deformed rocks, *Tectonophys.*, **24**, 115–131.

Stacey, F. D., 1963. The Physical theory of rock magnetism', *Adv. Phys.*, **12**, 45–133.

Stacey, F. D. & Banerjee, S. K., 1974. *The Physical Principles of Rock Magnetism*, Elsevier, Amsterdam.

Stephenson, A., 1980. A gyroremanent magnetization in anisotropic magnetic material, *Nature*, **284**, 49–51.

Stephenson, A., 1981. Gyromagnetic remanence and anisotropy in single-domain particles, rocks, and magnetic recording tape, *Phil. Mag. B*, **44**, 635–664.

Stephenson, A., 1983. Changes in direction of the remanence of rocks produced by stationary alternating field demagnetization, *Geophys. J. R. astr. Soc.*, **73**, 213–239.

Stephenson, A. & Collinson, D. W., 1974. Lunar magnetic field palaeointensities determined by an anhysteretic remanent magnetization method, *Earth planet. Sci. Lett.*, **23**, 220–228.

Uyeda, S., Fuller, M. D., Belshé, J. C. & Girdler, R. W., 1963. Anisotropy of magnetic susceptibility of rocks and minerals, *J. geophys. Res.*, **68**, 279–291.

Downloaded from https://academic.oup.com/gji/article/84/1/185/593598 by guest on 21 August 2022